Supporting Information

Molecular mechanisms of chromium(III) immobilization by organo-ferrihydrite coprecipitates: The significant roles of ferrihydrite and carboxyl

Jianjun Yang[a,b]*,Xing Xia[a], Jin Liu[c], Jian Wang[d], Yongfeng Hu[d]

[a] Institute of Environment and Sustainable Development in Agriculture, Chinese Academy of Agricultural Sciences, Beijing 100081, China

[b] Key Laboratory of Argo-Environment, Ministry of Agriculture and Rural Affairs, Beijing 100081, China

[c] College of Agronomy and Biotechnology, China Agricultural University, Beijing 100094, China

[d] Canadian Light Source Inc., University of Saskatchewan, Saskatoon, S7N 2V3 Canada

Number of pages: 16

Number of tables: 5

Number of figures: 13

***Corresponding author:** yangjianjun@caas.cn, phone: 86-10-82015996.

1 Cr(III) adsorbed on Ferrihydrite (Fh) (Fh-Cr(III)), amorphous $Cr(OH)_3$ ($Cr(OH)_3$(am)) and organo-Cr(III) complexes (OC-Cr(III)) synthesis

The Fh was synthesized following the method described by Schwertmann and Cornell.[1] Briefly, the pH of 0.1 M $FeCl_3$ solution was adjusted to ~7 using a 0.1 M NaOH solution. After shaking for 24 h, the suspension was separated by centrifugation and the paste was washed twice to remove residual ions using Mili-Q water, and then freeze-dried for 48 h. The adsorption of Cr(III) to Fh was conducted by mixing 20 mg dried Fh with 20 mL 0.1 mM $CrCl_3$ solution in a 50 ml plastic tube. To prevent the possible formation of $Cr(OH)_3$ precipitation on the surface of Fh, a low pH of 4.5 was kept during the adsorption experiment. The sorption result showed that the 80% Cr(III) was removed from solution to Fh. According to the Cr(III) binding sites density of Fh (1.3 sites nm^{-2}) and the specific surface area (SSA) of Fh (305.05 m^2 g^{-1}) (Table S2, IS), ~11.6% Cr(III) binding sites of Fh were occupied by Cr(III), which suggested no $Cr(OH)_3$ surface precipitates formation in the product.[2] Therefore, the adsorption product should be theoretically predominant as Fh-Cr(III). However, Cr(III) surface hydroxyl polymers, having a similar structure with $Cr(OH)_3$, most probably presented on the Fh surface instead of isolated Cr atoms according to previous study.[2]

The synthesis method of amorphous chromium(III) hydroxide ($Cr(OH)_3$(am)) was same as the Fh. The $Cr(OH)_3$(am) rather than crystalline $Cr(OH)_3$ was selected as a standard reference because NaOH solution was used to adjust pH, and thus no crystalline $Cr(OH)_3$ formed in this study.[3] This was because the synthesis of crystalline $Cr(OH)_3$ required NH_3H_2O or KOH solutions.[4, 5]

The OC-Cr(III) was made by mixing 60 mg L^{-1} rice or rape DOC with 0.1 mM $CrCl_3$ at

pH of 4.5. The paste of OC-Cr(III) was obtained by centrifugation and washed twice with Mili-Q water to remove residual DOC or Cr(III). Then the paste was freeze-dried for XANES measurements. Since there is little difference of Cr K-edge XANES between rice and rape derived OC-Cr(III) (data are not shown). In this study, we chose rice derived OC-Cr(III) as a standard compound for further bulk XANES analysis.

2 XRD, SEM-EDS and BET measurements

All the OFC samples were freeze-dried and ground into powders for further characterization. XRD analysis was conducted at ambient conditions using Cu-Kα radiation produced with 40 kV and 30 mA electron beam. SEM-EDS analysis was performed using scanning electron microscope (SEM) (Zeiss Auriga Compact) in conjunction with energy dispersive X-ray spectroscopy (EDS) (X-MAX80).The SSA of the OFC was determined through measurements of N_2 gas adsorption isotherms after degassing.

3 C K-edge and Cr L-edge XANES

Bulk C K-edge XANES spectra were collected at the beamline BL08U at the Shanghai Synchrotron Radiation Facility (SSRF) in China.[6, 7] The two DOC stocking solutions were freeze-dried and the deposited samples were ground into powders. Then the OC powders and oxalic acid reference were attached onto Cu tape fixed by a holder for spectral collection in the total electron yield mode. To improve the signal-to-noise ratio, at least of two scans were conducted for each sample and then all the spectra were processed using Athena software.[8]

4 STXM data analysis

The Stack Analyze, aXis2000 software package were applied for the alignment of image sequence and spectra processing. After alignment, the equation: optical density (OD) = ln(*I0/I*)

was used to convert data to optical density, where *I* referred to the flux passed through the sample, and the *I0* (incident flux) was obtained by measuring an empty region without samples. The C, Fe and Cr distribution maps were obtained by subtracting average images at the pre-edge range from the averaged images for each element. The energy ranges were listed in Table S5. The C K-edge, Cr and Fe $L_{3,2}$-edge XANES spectra of the selected regions of interest (ROIs) of the sorption and co-precipitation experiments were derived using aXis2000 software, and plotted using origin 8.5 for fingerprint analysis. PCA-Cluster analysis of the sorption and co-precipitation samples were processed using PCA GUI (1.1.1) software.

5 Impact of pH increase on Cr(III) precipitation in $CrCl_3$ solution

The solution of 0.1 mM $CrCl_3$ was prepared in two replicates by dissolving $CrCl_3$ chemicals in 10 mM NaCl solution, and the pH of 0.1 mM $CrCl_3$ was determined. Then NaOH solution was used to adjust the pH of the $CrCl_3$ solution to the experimental pH (5.5). After shaking at 200 rpm for 24 hours at 25 ℃, the $CrCl_3$ solution were centrifuged at 5, 000 rpm for 15 mins, and the supernatants of the $CrCl_3$ solution were filtrated using 0.45 μm membrane filters to determine the concentrations of soluble Cr using ICP-OES (Agilent 5110). The removal of the Cr in the solution was calculated by the difference between the initial added Cr and the remaining Cr in the supernatants.

6 Additional results

Table S1. The contents of interested elements in the rice and rape straw-derived DOC.

	C (mg L^{-1})	N (mg L^{-1})	Al (mg L^{-1})	Ca (mg L^{-1})	Fe (mg L^{-1})	K (mg L^{-1})	Mn (mg L^{-1})	P (mg L^{-1})	S (mg L^{-1})
Rice	2476.5	1364.1	0.9	6.1	3.7	1677.2	44.9	36.2	77.6
Rape	2077.1	1390.5	0.2	214.4	0.5	1834.7	0.4	88.8	282.3

Table S2. Final Fe/C molar ratios and SSA of OFC formed under different initial solution Fe/C molar ratios.

DOC	Initial Fe/C in solution	Fe/C in OFC[a]	SSA ($m^2 g^{-1}$)
-	control	-	305.05
Rice	10	11.31	317.06
	0.5	0.53	0.15
	0.1	0.02	1.08
Rape	10	9.94	294.02
	0.5	0.52	-[b]
	0.1	0.01	1.01

[a]The Fe/C molar ratio in OFC was calculated through the difference of Fe, C concentrations in solution before and after reactions.

[b] The SSA is under the detection limit with our sample weight.

Table S3. Results of the first four components obtained from PCA analysis on Cr K-edge XANES spectra of the studied OFC samples.

Components	Eigenvalue	Variation	Accumulated variation	IND
Component 1	113.8	0.925	0.925	0.0295
Component 2	7.091	0.057	0.983	0.0058
Component 3	0.901	0.007	0.990	0.0043
Component 4	0.479	0.003	0.994	0.0032

Table S4. Linear combination fitting results of the Cr K-edge XANES spectra of the OFCs from the sorption and co-precipitation experiments under different Fe/C molar ratios. The standard deviation is shown in the bracket

Sample	Goodness of fit		Percentage of Cr(III) species		
	R factor	χ^2	Fh-Cr(III)	OC-Cr(III)	$Cr(OH)_3$
Sor_control	0.0003	0.0395	90 (3)		10 (3)
Sor_Ri_0.5	0.0006	0.0815	68 (6)	32 (6)	
Sor_Ra_0.5	0.0005	0.0739	52 (6)	48 (6)	
Sor_Ri_0.1	0.0003	0.0483	27 (5)	73 (5)	

Sor_Ra_0.1	0.0002	0.0335	62 (4)	38 (4)	
Cop_control	0.0014	0.1903	77 (7)		23 (7)
Cop_Ri_0.5	0.0017	0.2254	75 (11)	25 (11)	
Cop_Ra_0.5	0.0050	0.6034	73 (17)	27 (17)	
Cop_Ri_0.1	0.0011	0.1436	70 (8)	30 (8)	
Cop_Ra_0.1	0.0005	0.0779	53 (6)	47 (6)	

Table S5. Pre-edge energy and edge-energy ranges used for the generation of average stack maps using STXM data.

Element	Absorption edge	Pre-edge energy stack range (eV)	Edge energy stack range (eV)
Total C	K	280-282	300-320
Aromatic C		280-282	285.2-285.8
Aliphatic C		280-282	287.1-287.9
Carboxylic C		280-282	288.3-288.9
Fe	L	700-704	709.0-709.8
Cr	L	570-572	577.2-578.1

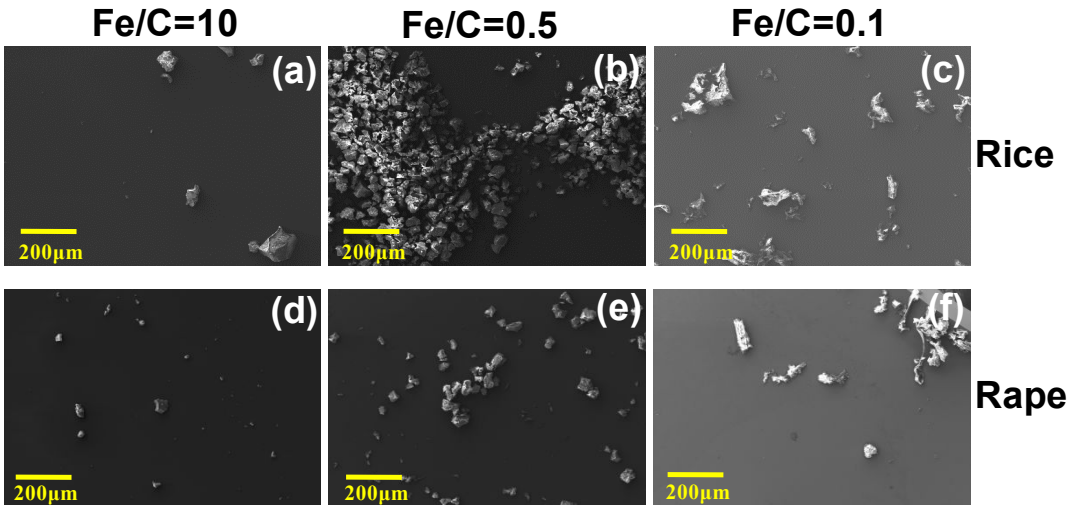

Figure S1. SEM images of the OFC under different Fe/C molar ratios at a relative large scale.

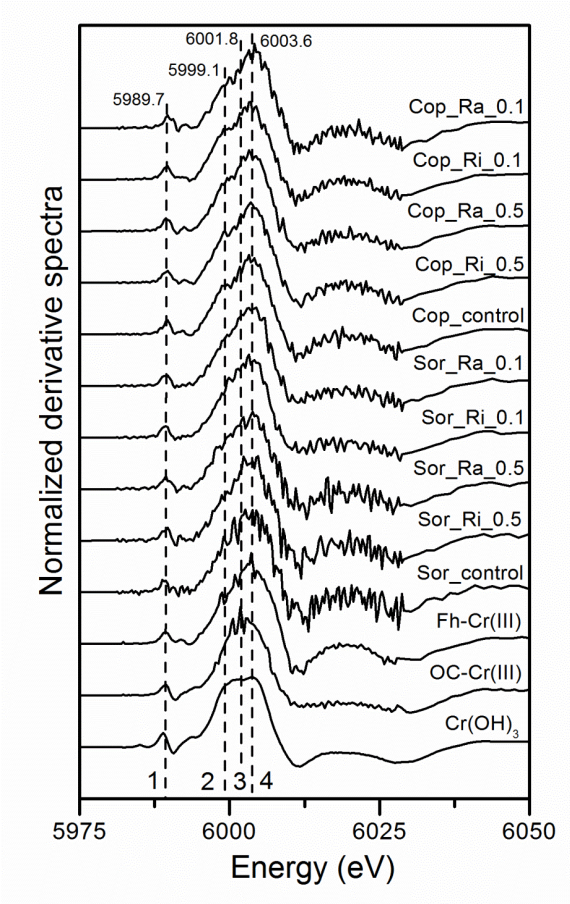

Figure S2. The first derivative spectra of Cr K-edge XANES spectra of OFC and standards (a). Sor_Ri_10 or Cop_Ra_10 refer to the OFC with Cr produced from adsorption or co-precipitation in the presence of DOCri or DOCra at the Fe/C molar ratio of 10, respectively, the others were named similarly.

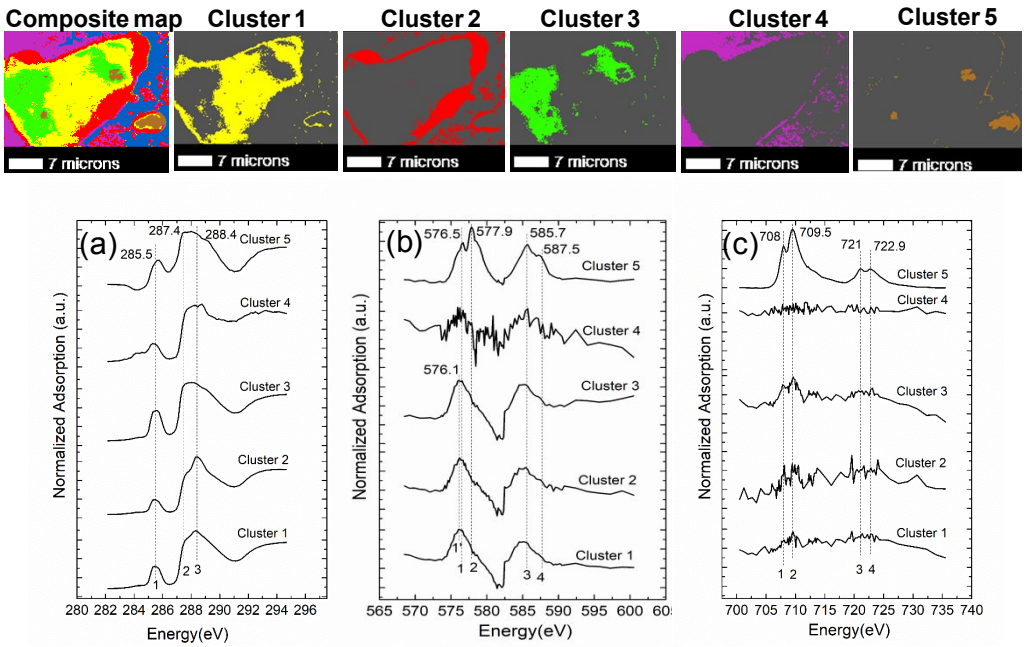

Figure S3. The PCA-cluster results of the sorption OFC sample synthesized using rice-derived DOC under the Fe/C molar ratio of 0.1(Sor_Ri_0.1). Corresponding C K-edge, Cr and Fe $L_{3,2}$-edge XANES spectra of each cluster identified is shown in (a), (b) and (c), respectively.

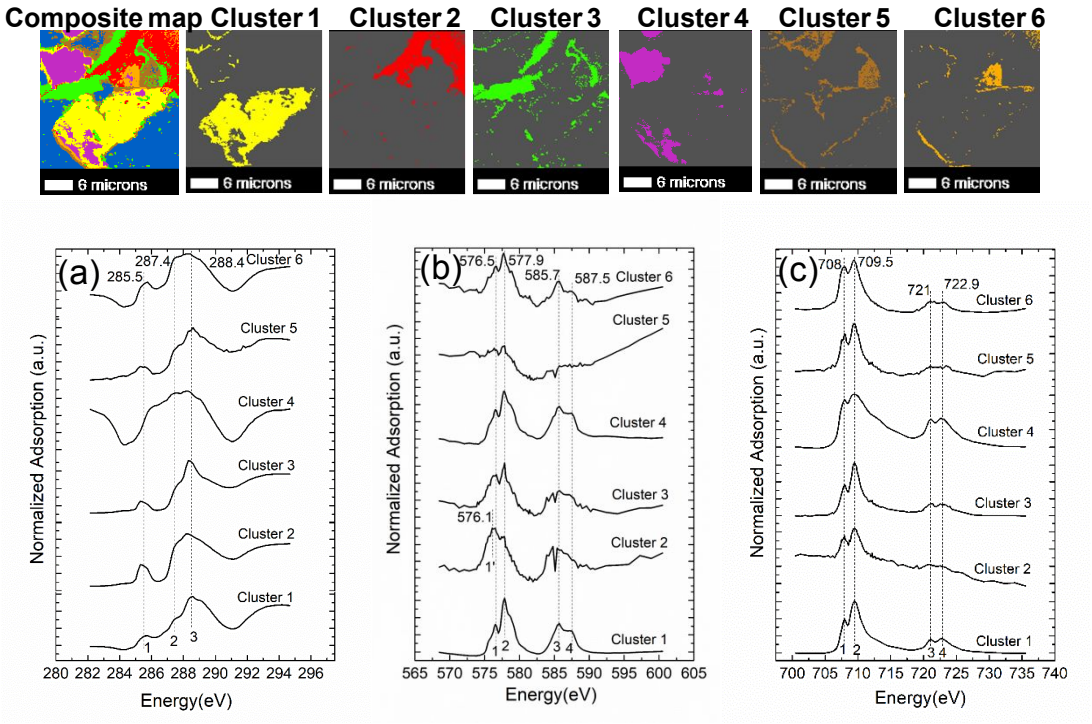

Figure S4. The PCA-cluster results of the sorption OFC sample synthesized using rape-derived DOC under the Fe/C molar ratio of 0.1 (Sor_Ra_0.1). Corresponding C K-edge, Cr and Fe $L_{3,2}$-edge XANES spectra of each cluster identified is shown in (a), (b) and (c), respectively.

.

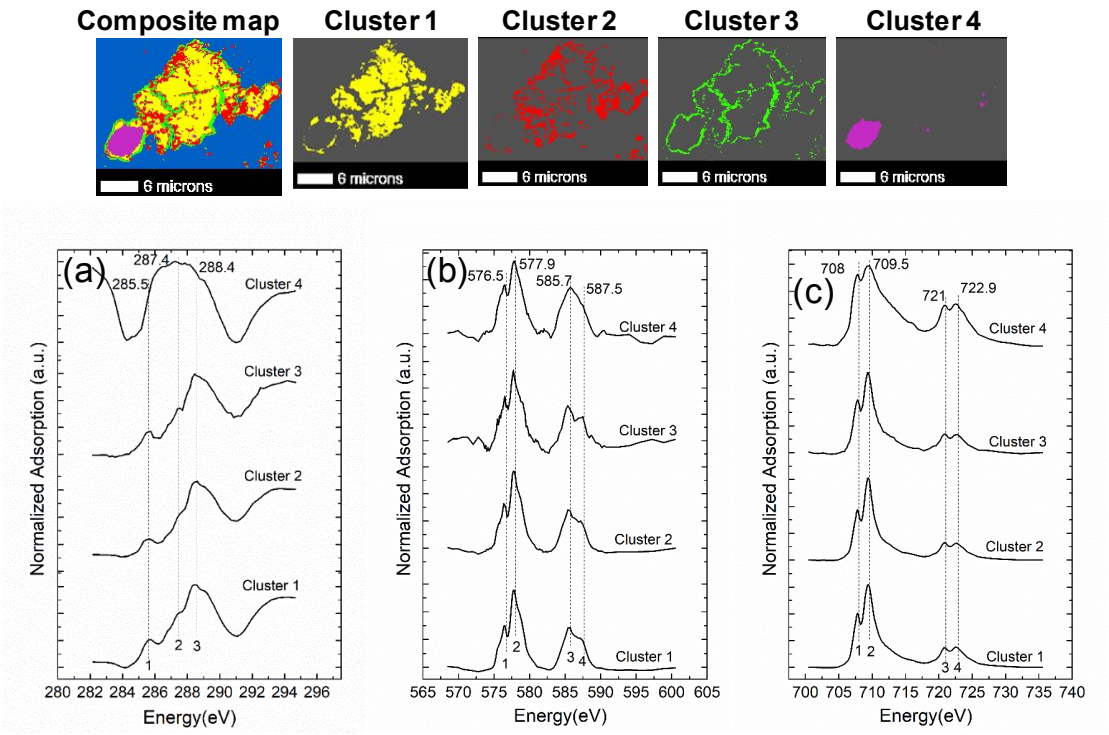

Figure S5. The PCA-cluster results of the co-precipitation OFC sample synthesized using rice-derived DOC under the Fe/C molar ratio of 0.1 (Cop_Ri_0.1). Corresponding C K-edge, Cr and Fe $L_{3,2}$-edge XANES spectra of each cluster identified is shown in (a), (b) and (c), respectively.

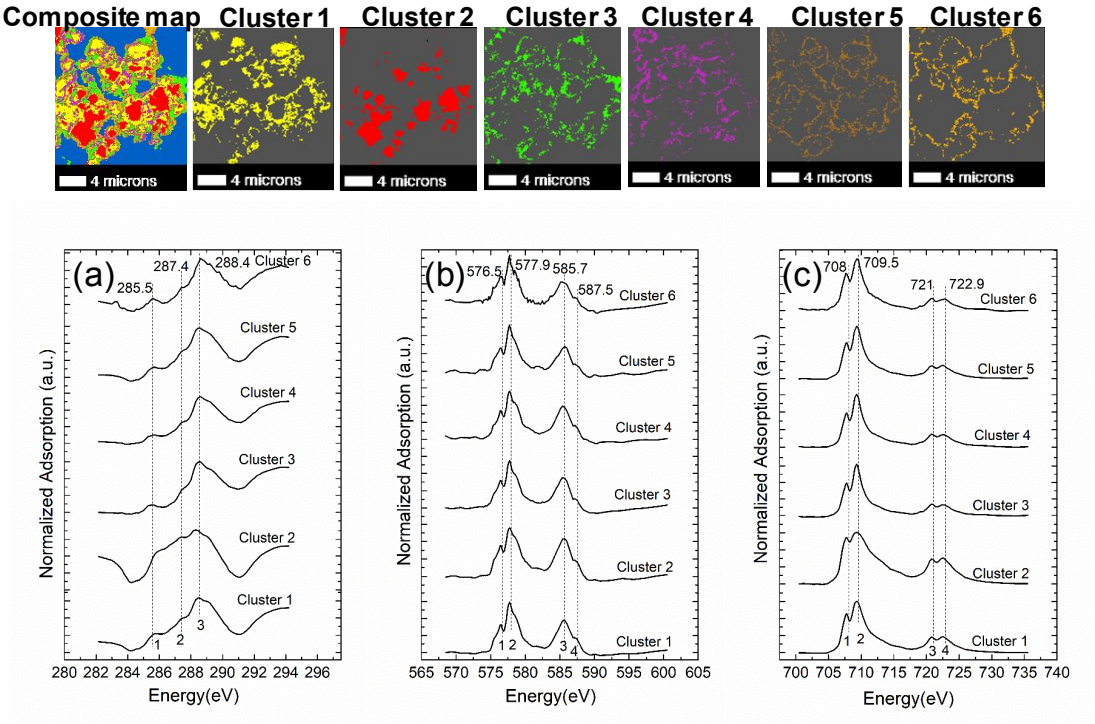

Figure S6. The PCA-cluster results of the co-precipitation OFC sample synthesized using rape-derived DOC under the Fe/C molar ratio of 0.1 (Cop_Ra_0.1). Corresponding C K-edge, Cr and Fe $L_{3,2}$-edge XANES spectra of each cluster identified is shown in (a), (b) and (c), respectively.

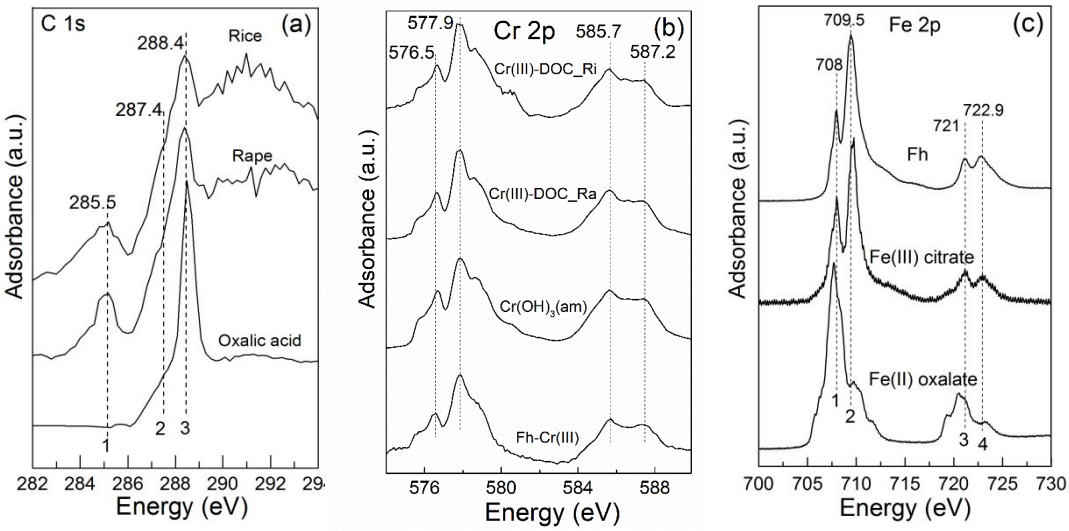

Figure S7. The XANES spectra at the C K-edge of rice (DOC_Ri) and rape derived DOC (DOC_Ra) (a), at the Cr $L_{3,2}$-edge of organo-Cr(III) complexes formed using DOC_Ri and DOC_Ra, amorphous $Cr(OH)_3$(am) and Cr(III) adsorbed on Fh (Fh-Cr(III)) (b) and Fe $L_{3,2}$-edge of ferrihydrite (Fh), Fe(III) citrate and Fe(II) oxalate (c) from previous studies, [9, 10] respectively.

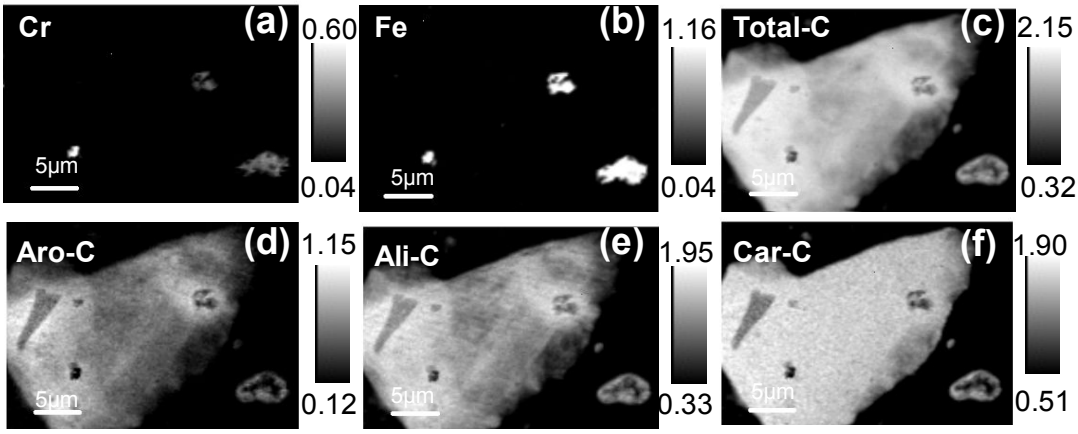

Figure S8. Submicro-scale distribution of Cr (a), Fe (b), total C (c, Total-C), aromatic carbon (d, Aro-C), aliphatic carbon (e, Ali-C) and carboxylic carbon (f, Car-C) in the sorption OFC sample, synthesized using rice-derived DOC under the Fe/C molar ratio of 0.1(Sor_Ri_0.1) determined by STXM.

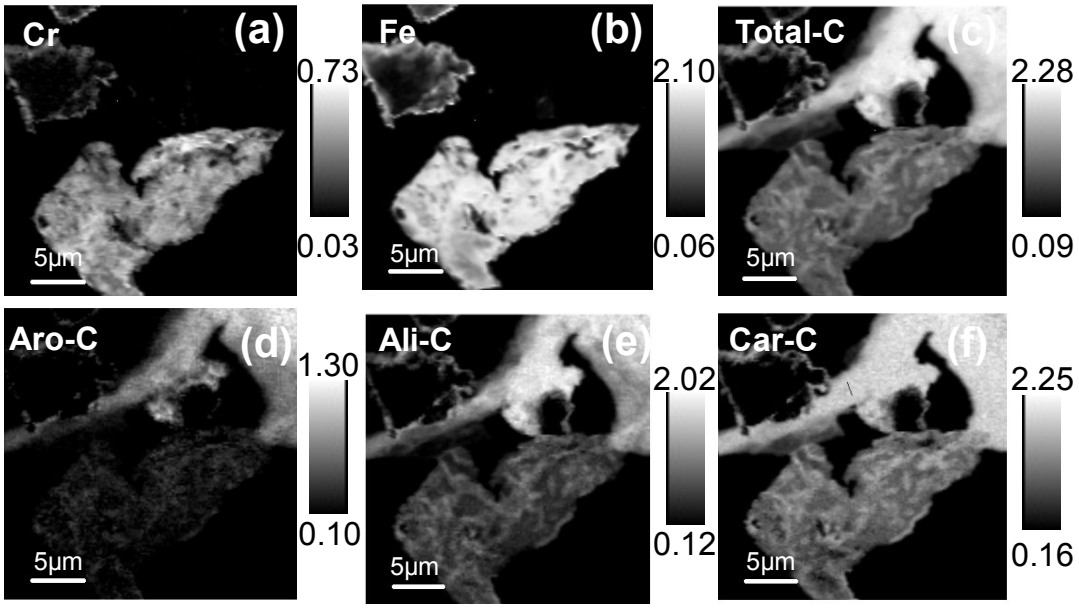

Figure S9. Submicro-scale distribution of Cr (a), Fe (b), total C (c, Total-C), aromatic carbon (d, Aro-C), aliphatic carbon (e, Ali-C) and carboxylic carbon (f, Car-C) in the sorption OFC sample, synthesized using rape-derived DOC under the Fe/C molar ratio of 0.1 (Sor_Ra_0.1) determined by STXM.

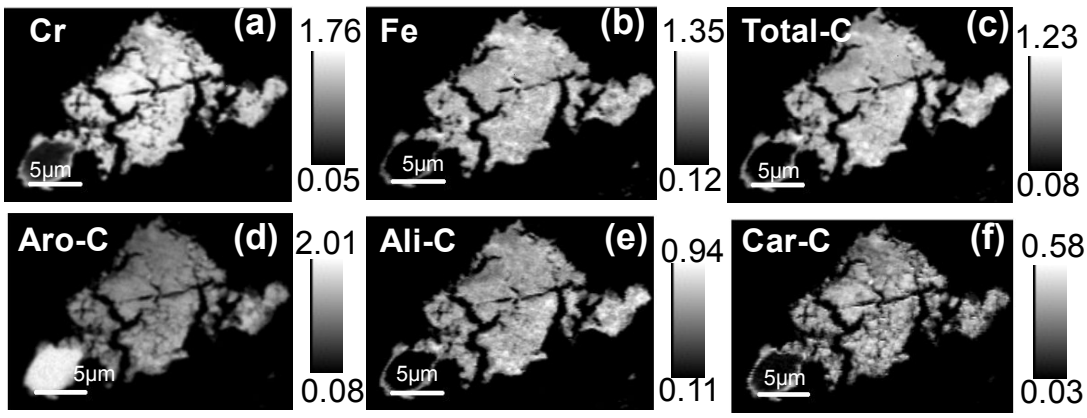

Figure S10. Submicro-scale distribution of Cr (a), Fe (b), total C (c, Total-C), aromatic carbon (d, Aro-C), aliphatic carbon (e, Ali-C) and carboxylic carbon (f, Car-C) in the co-precipitation OFC sample, synthesized using rice-derived DOC under the Fe/C molar ratio of 0.1 (Cop_Ri_0.1) determined by STXM.

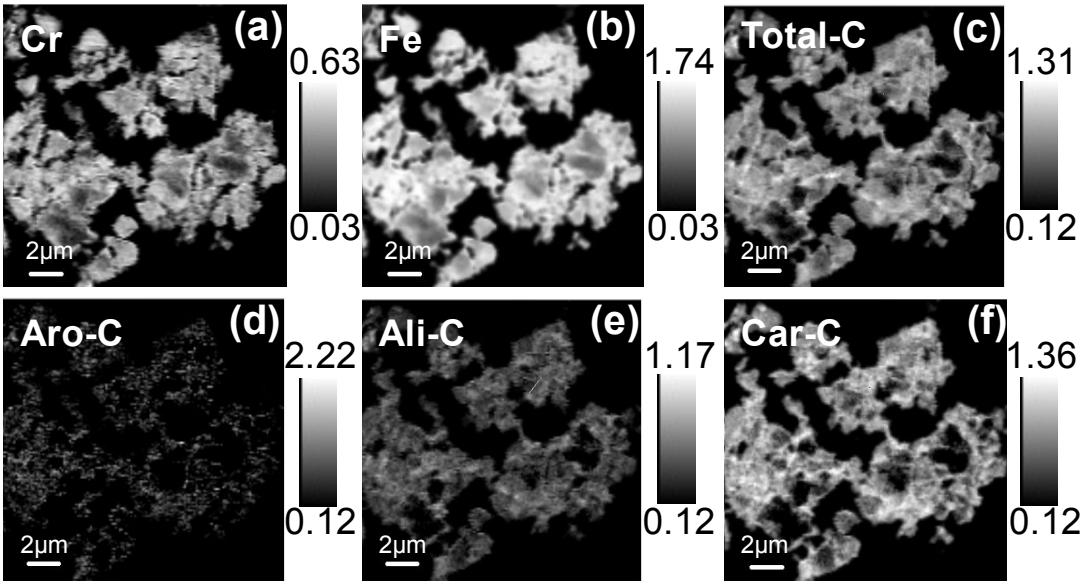

Figure S11. Submicro-scale distribution of Cr (a), Fe (b), total C (c, Total-C), aromatic carbon(d, Aro-C), aliphatic carbon (e, Ali-C) and carboxylic carbon (f, Car-C) in the co-precipitation OFC sample, synthesized using rape-derived DOC under the Fe/C molar ratio of 0.1 (Cop_Ra_0.1) determined by STXM.

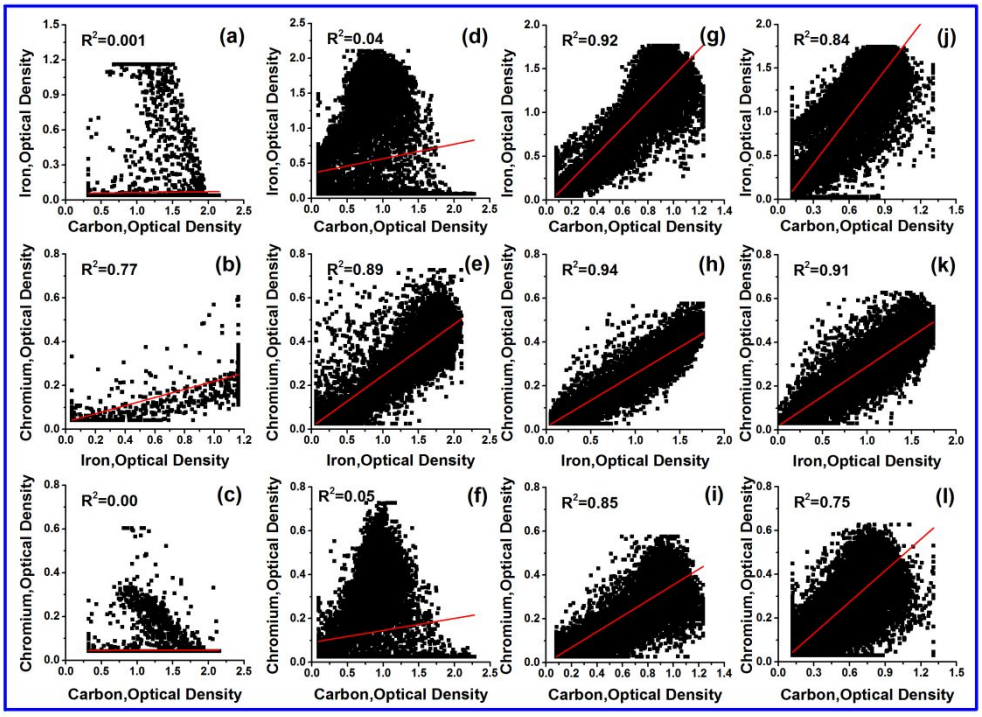

Figure S12. The elemental optical density correlation plots among C, Fe, and Cr for the sorption samples synthesized under the Fe/C molar ratio of 0.1 using rice- (Sor_Ri_0.1, a-c)

and rape-derived DOC (Sor_Ra_0.1, d-f), as well as the co-precipitation OFC samples under the Fe/C molar ratio of 0.1 using rice- (Cop_Ri_0.1, g-h) and rape-derived DOC (Cop_Ra_0.1, j-l), respectively.

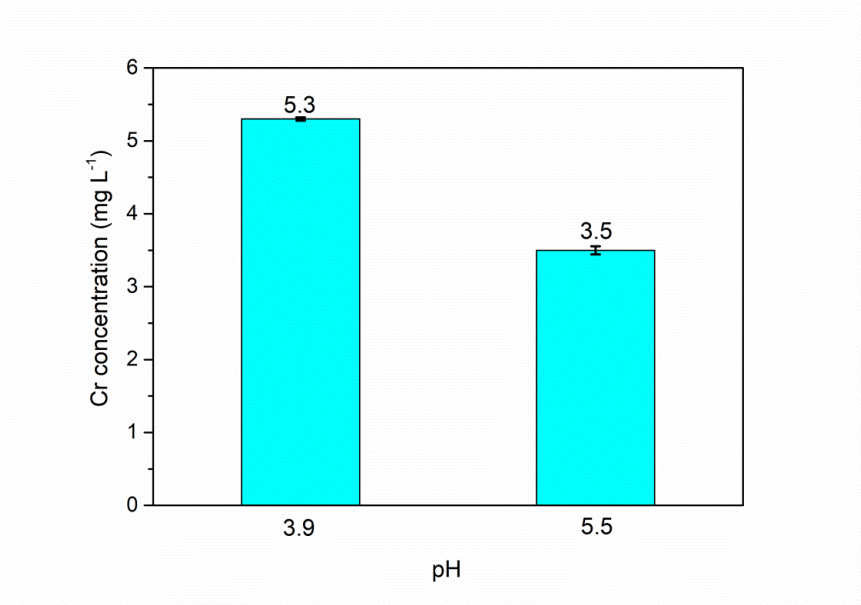

Figure S13. Concentrations of Cr in the supernatants of solutions containing 0.1 mM $CrCl_3$ and 10 mM NaCl at pH 3.9 (mean value, 5.3) and pH 5.5 (mean value, 3.5) after 24 h shaking.

References

1. Cornell, R. M.; Schwertmann, U., The iron oxides: structure, properties, reactions, occurrences and uses. Second Edition[M]. 2004.

2. Charlet, L.; Manceau, A. A., X-ray absorption spectroscopic study of the sorption of Cr(lll) at the oxide-water interface II. Adsorption, coprecipitation, and surface precipitation on hydrous ferric oxide. *J Colloid Interf. Sci* **1992,** *148*, (2), 443-458.

3. Zhang, H. L.; Liang, S. T.; Luo, M. T.; Ma, M. G.; Fan, P. P.; Xu, H. B.; Li, P.; Zhang, Y., Preparation and color performance control of Cr2O3 green pigment through thermal decomposition of chromium hydroxide precursor. *Mater. Lett* **2014,** *117*, 244-247.

4. Papassiopi, N.; Pinakidou, F.; Katsikini, M.; Antipas, G. S. E.; Christou, C.; Xenidis, A.; Paloura, E. C., A XAFS study of plain and composite iron(III) and chromium(III) hydroxides. *Chemosphere* **2014,** *111*, 169-176.

5. Laubengayer, A. W.; McCune, H. W., New crystalline phases in the system

chromium(III) oxide—water[1]. *J. Am. Chem. Soc* **1952,** *74*, (9), 2362-2364.

6. Yang, J.; Zhu, S.; Zheng, C.; Sun, L.; Liu, J.; Shi, J., Impact of S fertilizers on pore-water Cu dynamics and transformation in a contaminated paddy soil with various flooding periods. *J Hazard Mater* **2015,** *286*, 432-9.

7. Liu, J.; Yang, J.; Zeng, X.; Wang, J.; Sparks, D., Fe(III)-induced sequestration of citric acid on kaolinite surface probed by STXM-NEXAFS spectroscopy. *Acta Chim. Sinica* **2017,** *75*, (6), 617-620.

8. Ravel, B.; Newville, M., ATHENA, ARTEMIS, HEPHAESTUS: data analysis for X-ray absorption spectroscopy using IFEFFIT. *J. Synchrotron. Radiat* **2005,** *12*, 537-541.

9. Yang, J.; Wang, J.; Pan, W.; Regier, T.; Hu, Y.; Rumpel, C.; Bolan, N.; Sparks, D., Retention mechanisms of citric acid in ternary kaolinite-Fe(III)-citrate acid systems using Fe K-edge EXAFS and L-3,L-2-edge XANES spectroscopy. *Sci. Rep* **2016,** *6*.

10. Yang, J.; Wang, J., Radiation chemistry of molecular compounds and polymers by soft X-ray spectroscopy and microscopy. *Can. J. Chem* **2017,** *95*, (11), 1191-1197.